Potential competition between marine heterotrophic prokaryotes and autotrophic picoplankton for nitrogen substrates

Wenchao Deng [ID],[1,2] Shanlin Wang,[1,3] Xianhui Wan,[1] Zhenzhen Zheng,[4] Nianzhi Jiao,[1,3] Shuh-Ji Kao [ID],[1,3]
Jefferson Keith Moore,[5] Yao Zhang [ID][1,3]*

[1]State Key Laboratory of Marine Environmental Sciences, Xiamen University, Xiamen, China
[2]College of the Environmental and Ecology, Xiamen University, Xiamen, China
[3]College of Ocean and Earth Sciences, Xiamen University, Xiamen, China
[4]State Key Laboratory of Marine Resource Utilization in South China Sea, Hainan University, Haikou, China
[5]Department of Earth System Science, University of California, Irvine, California

Abstract

Heterotrophic prokaryotes have the capacity to uptake inorganic nitrogen (N) substrates. However, it remains unclear what the potential competition is between heterotrophic prokaryotes and autotrophic plankton for N in the ocean, which would shunt the flow of N supporting primary production. To date, it has been difficult to distinguish heterotrophic prokaryotic N uptake from that of autotrophic picoplankton, especially in oligotrophic oceans dominated by cyanobacteria. We carried out field-based DNA stable isotope probing incubation experiments in the South China Sea combining measurements of uptake rates of ammonium, nitrate, nitrite, and urea to estimate the taxon-specific potential N assimilation. The results indicate that phylogenetically diverse heterotrophic prokaryotes significantly incorporated multiple N sources, contributing approximately 17–41% and 19–55% of total N uptake potential in the euphotic zone of the South China Sea continental shelf and open ocean, respectively, potentially competing with cyanobacteria (mainly *Prochlorococcus*). Notably, heterotrophic prokaryotes made a higher contribution to bulk uptake of nitrate in the incubation systems of the open ocean relative to regenerated N, and thus there was a tendency to overestimate the *f*-ratio. Extrapolating our results to the oligotrophic, low-latitude ocean via a global model suggests the *f*-ratio would decrease ~ 18%. This suggests a more complicated biogeochemical role of heterotrophic prokaryotes in the biological carbon pump than hitherto assumed, with important implications for N and carbon cycling in the vast open ocean.

Nitrogen (N) limits the primary productivity of autotrophic plankton that, together with subsequent carbon export into deeper ocean waters, drives marine carbon sequestration by the so-called biological pump. Ammonium (NH_4^+), nitrate (NO_3^-), nitrite (NO_2^-), and urea are the major nitrogenous substrates ("N substrate[s]" hereafter only refers to these four

Additional Supporting Information may be found in the online version of this article.

substrates) supporting oceanic primary production; thus, measuring their uptake is of primary concern (Mulholland and Lomas 2008). Nitrogen imported into the euphotic zone supports new production, which can be exported into the deep ocean (Eppley and Peterson 1979). The primary source of "new" N to the euphotic zone in the open ocean is thought to be upward diffusion and convection of NO_3^- (Dugdale and Goering 1967). Ammonium and urea are the main N compounds internally recycled within the system, supporting "regenerated" primary production (Dugdale and Goering 1967). Ammonium oxidation and assimilatory reduction of NO_3^- by phytoplankton are two dominant sources of NO_2^- in the euphotic zone (Lomas and Lipschultz 2006; Buchwald and Casciotti 2013) and, therefore, NO_2^- uptake can contribute to new or regenerated primary production.

Conventionally, autotrophic plankton are primary consumers of dissolved inorganic nitrogen (DIN) (NH_4^+, NO_3^-, NO_2^-) in the euphotic zone, while bacterial heterotrophs are primary consumers of organic compounds. However, the capacities of autotrophic plankton to use organic N as an N

source, such as urea, cyanate, and amino acids (Mulholland and Lomas 2008; Widner and Mulholland 2017), and heterotrophic bacteria to use DIN (Eppley et al. 1977; Middelburg and Nieuwenhuize 2000; Trottet et al. 2016) have been well recognized. Heterotrophic bacteria assimilate DIN when the N contained in organic matter is insufficient to support their growth (Middelburg and Nieuwenhuize 2000). Previous studies from nutrient-rich coastal and estuarine waters as well as from (sub)Arctic waters, using size fractionation or prokaryotic/eukaryotic metabolic inhibitors, have reported that heterotrophic bacterial assimilation of NH_4^+ and NO_3^- accounted for a significant but variable fraction (< 5% to > 90%) of bulk uptake (Middelburg and Nieuwenhuize 2000; Bradley et al. 2010; Trottet et al. 2016). This variability can be caused by many reasons, such as the temporal and spatial variation of N species, light limitation of autotrophs, autotrophic and heterotrophic microbial composition, as well as the labile carbon availability for heterotrophic prokaryotes (Mulholland and Lomas 2008). Similarly, heterotrophic bacterial assimilation of urea has also been reported to account for a widely variable fraction (< 10% to > 80%) of bulk urea uptake by the coastal and estuarine plankton community (Cho and Azam 1995; Middelburg and Nieuwenhuize 2000).

These studies provided solid evidence of heterotrophic bacterial N substrate assimilation potential; however, competition for DIN and urea between heterotrophic prokaryotes and autotrophic plankton remains unclear. This is important for the estimation of *f*-ratio, which is usually a measure of NO_3^- uptake to total N ($NO_3^- + NH_4^+ +$ urea) uptake and used to assess the new production and biological pump efficiency. Especially in open oceans, cyanobacteria *Prochlorococcus* and *Synechococcus* are the dominant primary producers, which cannot be distinguished from heterotrophic bacteria and archaea using either size fractionation (Bradley et al. 2010; Klawonn et al. 2019) or prokaryotic and eukaryotic metabolic inhibitors (Middelburg and Nieuwenhuize 2000; Fouilland et al. 2007; Trottet et al. 2016). It remains difficult to distinguish which group or cells are taking up which compounds in bulk substrate uptake bioassays (Mulholland and Lomas 2008). Using ^{15}N-based DNA stable isotope probing (DNA-SIP) linking the identity of active microorganisms with their function (Radajewski et al. 2000), previous studies have identified diverse heterotrophic bacteria incorporating N substrates in the West Florida Shelf (Wawrik et al. 2012) and the Southern California Bight (Morando and Capone 2018), as well as offshore of Barrow in the Arctic (Connelly et al. 2014). The competition between heterotrophic prokaryotes and autotrophic plankton was not evaluated quantitatively, however, and there were very few cyanobacteria in these coastal or high-latitude regions.

The heterotrophic bacterial assimilation of N substrates complicates our understanding of new and regenerated marine production. The *f*-ratio multiplied by primary production (estimated from ^{14}C-assimilation) has long been used to

estimate new production (Eppley and Peterson 1979), on the assumption that only autotrophic plankton take up DIN and urea (Fouilland et al. 2007). Direct conversion of N to carbon by assuming Redfield ratio stoichiometry (C = N × 6.6 by moles; Dugdale et al. 1989) has also conventionally been used to obtain NO_3^--based new production (Chen 2005; Shiozaki et al. 2013). In addition, N_2 fixation has recently been recognized to be important for new production, and hence the corrected *f*-ratio including N_2 fixation is proposed (Shiozaki et al. 2013). However, failing to consider heterotrophic prokaryotic assimilation of NO_3^- and regenerated N can bias the *f*-ratio in environments.

To resolve this primary concern, we performed field-based incubation experiments of nano- and pico-sized microbial communities (< 20 μm and < 3 μm, respectively) in the South China Sea. ^{15}N-labeled NH_4^+, NO_3^-, NO_2^-, or urea was added in the incubation systems and microbial ^{15}N-DNA and ^{14}N-DNA analyses were carried out. In addition, N isotopic compositions ($\delta^{15}N$) of the community in incubated seawater were measured to estimate potential N uptake rates. Taken together, these analyses revealed taxon-specific capabilities for DIN and urea utilization, and assessed the potential influence of heterotrophic prokaryotic assimilation of N on *f*-ratio estimates.

Materials and methods

Field sampling and biogeochemical parameter measurements

About 120 L of seawater was collected for the incubation experiments from the 20% and 1% photosynthetically active radiation (PAR) depths at the typical continental shelf site I1 (20 and 70 m water depth) and open ocean site SEATS (50 and 100 m water depth) (Supporting Information Fig. S1) by a Sea-Bird conductivity-temperature-depth system (SBE 9/11 plus) equipped with 12-liter Niskin bottles during a research cruise in the South China Sea in November to December 2016. Meanwhile, 2 L and 500 mL of seawater were collected on a 0.22-μm pore size polycarbonate filter (Millipore) and a precombusted (4 h at 500°C, Cherrier et al. 1996) 0.3-μm pore size glass fiber filter (Advantec) at each depth for in situ community DNA extraction and microbial ^{15}N content measurements, respectively. The polycarbonate filters were flash-frozen in liquid N and subsequently stored at −80°C and the glass fiber filters were frozen at −20°C until laboratory analysis. Seawater samples for flow cytometry were prefiltered through 20 μm mesh to remove large particles and zooplankton, added to glutaraldehyde (0.5% final concentration), incubated at 4°C for 15 min in the dark, flash-frozen in liquid N, and then stored at −80°C until laboratory analysis (Zhang et al. 2008). Seawater samples for inorganic nutrient and urea concentration measurements were collected into 150-mL acid-washed, seawater-rinsed, high-density polyethylene Nalgene bottles and acid-washed, precombusted (450°C for 4 h) 50-mL

brown glass vials, respectively. These samples were then stored at $-20°C$ until laboratory analysis.

Temperature, salinity, and depth were obtained from the conductivity-temperature-depth system (SBE 9/11 plus). PAR and total chlorophyll a (Chl a) fluorescence were tested using a PAR sensor (LI-193, Li-Cor Biosciences) and a SeaTech flash fluorometer, respectively. Total microbial abundance was determined using a BD Accuri C6 flow cytometer by staining with 1×10^{-4} SYBR Green I (v/v, final concentration, Molecular Probes) (Marie et al. 2001). Abundances of *Prochlorococcus*, *Synechococcus*, and pico/nano-eukaryotes were determined using an Epics Altra II flow cytometer (Beckman Coulter) (Zhang et al. 2008). Nitrate and NO_2^- concentrations were measured by the colorimetric method with a four-channel continuous Flow Technicon AA3 Auto-Analyzer (Bran-Lube GmbH) (Han et al. 2012). Ammonium concentrations were measured using the fluorometric method with a detection limit of 1.2 $nmol\,L^{-1}$ and precision of $\pm 3.5\%$ (Wan et al. 2018). Urea concentrations were measured using a 1-m long liquid waveguide capillary cell system (World precision Instruments) based on the colorimetric reaction with diacetyl monoxime; the detection limit was 1.2 $nmol\,L^{-1}$ (Chen et al. 2015).

Incubation experiments

Seawater collected for incubation was immediately filtered through $20\,\mu m$ mesh to remove zooplankton and obtain the $< 20\,\mu m$ community; half was subsequently filtered through $3\,\mu m$ polycarbonate filters to remove nanoplankton and obtain the $< 3\,\mu m$ community. Ten liters of each size-filtered seawater sample were incubated in polycarbonate bottles, which were previously washed with 10% HCl solution and in situ filtered seawater; and 98% of ^{15}N-labeled NH_4^+, NO_3^-, NO_2^-, or urea (Sigma-Aldrich) was added to a final concentration of 1.5 $\mu mol\,L^{-1}$ at 20% PAR depth and 2 $\mu mol\,L^{-1}$ at 1% PAR depth, which was similar to the previous SIP studies (Wawrik et al. 2012; Connelly et al. 2014; Morando and Capone 2016). Bottles without additions were regarded as blank controls. These bottles were incubated in an acrylic incubator simulating in situ temperature and light intensity with water flowing through a cooler and covered with neutral density screens (Lee Filters). All incubations were started about at 12:00 h and ended about at 00:00 h. Samples for microbial abundance and ^{15}N content were collected at the beginning of the experiment and after 36 h of incubation. The microbial community (8 L of the incubated seawater) was collected on $0.22\,\mu m$ polycarbonate filters with a suction pressure of <0.03 MPa after 36 h incubation. The filters were flash-frozen in liquid N and subsequently stored at $-80°C$ until laboratory analysis.

DNA extraction and CsCl density gradient ultracentrifugation

Microbial DNA was extracted using the phenol-chloroform-isoamyl alcohol method (Nercessian et al. 2005) and fluorometrically quantified using a Qubit dsDNA Assay Kit (Invitrogen) and Qubit 2.0 Fluorometer (Invitrogen). Cesium chloride (CsCl) density gradient ultracentrifugation and fractionation were performed according to published protocols (Neufeld et al. 2007; Connelly et al. 2014; Zhang et al. 2016) with minor modifications. Briefly, 1–3 μg of DNA was added to a CsCl solution to obtain a final density of ~ 1.703 $g\,mL^{-1}$. The solutions were injected into 5.1 mL Quick-Seal™ centrifuge tubes (Backman Coulter) and spun at $140,000 \times g$ in a VTi 65.2 rotor (Backman Coulter) at $20°C$ for 48 h under vacuum. Immediately after centrifugation, the density gradient solution was divided into 20 fractions by injecting mineral oil with a uniform flow of 255 $\mu L\,min^{-1}$ into the top of each centrifuge tube through a syringe pump (Braintree Scientific); the densities of all fractions were measured by a digital refractometer (Brix/RI-Chek, Reichert). The DNA in each fraction was precipitated by adding two volumes of polyethylene glycol solution (30% polyethylene glycol 6000, w/v, 1.6 $mol\,L^{-1}$ NaCl, and 20–40 μg of glycogen), resuspended in 35 μL of TE (10 $mmol\,L^{-1}$ TrisHCl, 1 $mmol\,L^{-1}$ EDTA, pH 8.0), and then quantified fluorometrically.

Quantitative polymerase chain reaction

Bacterial and archaeal 16S rRNA and eukaryotic 18S rRNA gene abundances in each fraction were quantified by quantitative polymerase chain reaction (qPCR) using primers Bac-338f and Bac-518r (Park and Crowley 2005), Arc-334f and Arc-806r (Wang et al. 2014), and Euk-345f and Euk-499r (Zhu et al. 2005), respectively, in a SmartChip Real-time PCR system (WaferGen Biosystems) according to Wang et al. (2014). In brief, 100 nL of the PCR mixture in each well ($1 \times$ LightCycler 480 SYBR Green I Master, 1 $mg\,mL^{-1}$ bovine serum albumin, 500 $nmol\,L^{-1}$ of each primer, and 21 nL template DNA) were dispensed into a 5184-wells chip using SmartChip Multisample Nanodispenser in 12 (assays) $\times$ 384 (samples) format. Each reaction mixture was run in triplicate with the program: initial enzyme activation at $95°C$ for 105 s, followed by 40 cycles of $95°C$ for 15 s, $55°C$ for 30 s, and $72°C$ for 30 s. Triplicate nontemplate reactions were run as negative controls on each chip. The efficiencies of qPCR amplification ranged from 89% to 101% with $R^2 > 0.99$. Archaeal ammonia monooxygenase subunit A (*amoA*) gene abundance was quantified using primers Arch-*amo*AFA (Beman et al. 2008) and Arch-*amo*AR (Francis et al. 2005) in a CFX 96™ real-time system (BIO-RAD). The reaction mixtures (20 μL) contained 10 μL of SYBR® Premix Ex Taq™ II (TakaRa), 5 μg of bovine serum albumin, 0.5 $\mu mol\,L^{-1}$ of each primer, and 1 μL of template DNA. The qPCR thermal cycling conditions were set according to Hu et al. (2011). The efficiencies of qPCR amplification ranged from 95% to 100% with $R^2 > 0.99$. The specificity of qPCR was confirmed by melting curve analysis and agarose gel electrophoresis. Ambiguous products were sequenced to confirm their veracity.

Bacterial and archaeal 16S rRNA gene sequence analysis

An equal volume of DNA solution from 1 to 3 continuous heavy (1.711–1.727 g mL^{-1}) or light (1.709–1.695 g mL^{-1}) CsCl gradient fractions that contained the most abundant bacterial or archaeal 16S rRNA gene copies (Supporting Information Figs. S2, S3) were mixed for high-throughput sequencing to obtain bacterial and archaeal populations that incorporated (heavy) and did not incorporate (light) ^{15}N-labeled substrates. The DNA from the ultralight density (~ 1.692 g mL^{-1}) fraction that contained the most abundant *amo*A gene copies in each sample was also subjected to archaeal 16S rRNA gene sequencing (Supporting Information Figs. S2, S3). The fractions selected for sequencing from all samples are shown in Supporting Information Table S1. Bacterial and archaeal V3–V4 hypervariable regions in 16S rRNA genes were amplified with the barcode sequences and universal primers Bac-341F (CCTACGGGNGGCWGCAG) and Bac-805R (GACTACHVGGGTATCTAATCC) (Herlemann et al. 2011) and Arc-349F (GYGCASCAGKCGMGAAW) and 806R (GGACTACVS GGGTATCTAAT) (Takai and Horikoshi 2000), respectively, and sequenced using an Illumina MiSeq PE300 at the Chinese National Human Genome Center (Shanghai).

Quality controlled sequences were classified and clustered into operational taxonomic units (OTUs) with a cutoff value of 0.03 using the Mothur software following standard operating procedures (www.mothur.org/wiki/MiSeq_SOP) (Kozich et al. 2013) as described by Zhang et al. (2016). Sequences in all samples were rarefied and subsampled to an equal number using the *sub.sample* command for normalization and further generated OTU relative abundance matrices based on which Bray-Curtis similarities between communities were calculated. Nonmetric multidimensional scaling ordinations were produced using Primer 5. One-way analysis of similarity with 999 permutations was performed to test the null hypothesis of no significant difference between clusters in the nonmetric multidimensional scaling charts. Representative sequences of OTUs were aligned using MEGA7 and the phylogenetic trees were constructed using the method of maximum likelihood. The normalized abundances of OTUs are shown as heat maps. The abundance of each OTU was calculated by multiplying the relative abundance with total 16S rRNA gene copy numbers in the sequenced fraction and then normalized by dividing the maximum total copy number among the sequenced fractions of each sample. Raw sequencing data of the bacterial and archaeal 16S rRNA gene are available at NCBI Sequence Read Archive under BioProject accession number PRJNA551971 with BioSample accession number SAMN12172468–SAMN12172550 (Bacteria) and SAMN12173333–SAMN12173433 (Archaea). The representative sequences used in bacterial and archaeal phylogenetic trees are under GenBank accession number MN145732–MN145848 and MN145685–MN145731, respectively.

Bulk N uptake rate

The δ^{15}N of particulate nitrogen (PN) was measured using the wet digestion method and the bacterial method according to previous studies (Knapp et al. 2005; Wan et al. 2018). Briefly, PN was oxidized to NO_3^- with purified persulfate oxidizing reagent and the NO_3^- concentration was measured by chemiluminescence for determining PN concentration. Then, the NO_3^- was converted to N_2O by using the denitrifier *Pseudomonas aureofaciens* (ATTC no. 13985) and the N_2O was introduced to a GasBench coupled to an isotope ratio mass spectrometer for measuring δ^{15}N. Nitrate isotope standards SGS 34, IAEA N3, and USGS 32 were used to calibrate the $\delta^{15}NO_3^-$ of the samples and the analytical precision was better than ± 0.2‰. The seawater from 3000 m water depth in the South China Sea was also analyzed as a laboratory working reference material for quality control (Wan et al. 2018). The bulk uptake rate of a N source in incubated seawater was calculated using Eqs. 1–3:

$$R_{sample} = \left(\frac{\delta^{15}N_{PN}}{1000} + 1 \right) \times R_{atmN_2} \tag{1}$$

$$n = \frac{R_{sample}}{R_{sample} + 1} \tag{2}$$

$$UR_{subs} = \frac{PN_t \times n_t - PN_0 \times n_0}{t} \times \frac{Ca_{subs} + Cs_{subs}}{Cs_{subs}} \tag{3}$$

where R_{sample} is the ratio of ^{15}N/^{14}N; R_{atmN_2} is the assumed ^{15}N content of standard atmospheric N ($= 0.365\%$) (Xu et al. 2017); n_t and n_0 are the atomic percentages of ^{15}N-PN at the end and beginning of an incubation; PN_t and PN_0 are the PN concentrations (i.e., concentrations of NO_3^- produced from oxidation of PN by persulfate oxidizing reagent) at the end and beginning of an incubation; Ca_{subs} and Cs_{subs} are the ambient and added substrate concentrations, respectively; t is the incubation time; and UR_{subs} is the bulk uptake rate of a N source in incubated seawater.

Concentration and N isotopic composition of dissolved organic N

To assess the potential impact of labeled organic materials release during N uptake, concentration and isotopic composition of dissolved organic N (DON) were measured at 0 and 36 h during the ^{15}N-NH$_4^+$ added incubations. To minimize influence of the added ^{15}N-NH$_4^+$ to DON measurement, the NH$_4^+$ was removed using the ammonia diffusion method (Holmes et al. 1998). Briefly, 20 mL of sample was transferred into 120 mL high-density polyethylene (Nalgene) bottles, pH of the sample was adjusted to ~ 12 by adding 6 mol L^{-1} of NaOH (ACS-grade, Merck) and was shaken vigorously at 25°C for 2 weeks. Sample was further purged by helium for 0.5 h to further remove any remaining NH$_3$. Then, the δ^{15}N of dissolved N was measured using the wet digestion method and the bacterial method as described above. To exam the NH$_4^+$ removal efficiency, ^{15}N-NH$_4^+$ was added to 20 mL of surface water from SEATS station to get a final concertation of

$2 \ \mu\text{mol N L}^{-1}$ and was treated as above. The NH_4^+ removal efficiency was obtained by comparing ^{15}N content between the digested SEATS surface water with and without $^{15}N\text{-}NH_4^+$ amendment, and it was $95.6\% \pm 3.7\%$ in our treatment ($n = 3$). Concentration and ^{15}N content of DON were calculated using Eqs. 4 and 5:

$$^{15}N_{DON} = \frac{C_{bulkN} \times n_{bulk} - C_{^{15}N-A} \times 0.04 \times 0.98 - C_{NO_X^-} \times n_{NO_X^-}}{C_{DON}} \quad (4)$$

$$C_{DON} = C_{bulkN} - C_A \times 0.04 - C_{NO_X^-} \quad (5)$$

where $^{15}N_{DON}$ is the ^{15}N fraction in DON (%); C_{DON}, C_{bulkN}, C_A, and C_{NO_X} are the DON, bulk N (after digestion), bulk NH_4^+, and NO_X^- (before digestion) concentrations, respectively; $C_{^{15}N-A}$ is the $^{15}NH_4^+$ concentration after the tracer amendment; and n_{bulk} and n_{NO_X} are the atomic percentages of ^{15}N in bulk N (after digestion) and NO_X^- (before digestion).

Taxon-specific N uptake

The difference in DNA density caused by ^{15}N isotope incorporation was estimated using the modified quantitative SIP method (Hungate et al. 2015). The total abundance of each taxon ($f_{s.T}$) and the average DNA density ($\bar{\rho}_{s.T}$) of taxon T in an entire density gradient were calculated using Eqs. 6 and 7, respectively:

$$f_{s.T} = \sum_{k=1}^{K} f_{s.k.T} \quad (6)$$

$$\bar{\rho}_{s.T} = \sum_{k=1}^{K} \rho_{s.k} \cdot \left(\frac{f_{s.k.T}}{f_{s.T}} \right) \quad (7)$$

where $f_{s.k.T}$ is the abundance of taxon T (T represents bacteria, archaea, or eukaryotes) in fraction k of density gradient from substrate s (s represents NH_4^+, NO_3^-, NO_2^-, or urea) added sample, and $\rho_{s.k}$ is the density of fraction k.

The percentage of DNA labeled by ^{15}N of each taxon ($P_{s.T}$) was calculated using Eq. 8:

$$P_{s.T} = \frac{\bar{\rho}_{s.T.Exp} - \bar{\rho}_{s.T.B}}{\triangle \rho} \times 100\% \quad (8)$$

where $\bar{\rho}_{s.T.Exp}$ and $\bar{\rho}_{s.T.B}$ are the average densities of DNA of taxon T from the experimental sample and blank control, respectively, and $\triangle \rho$ is the difference in density between $100\% \ ^{15}N$-labeled DNA and unlabeled DNA ($= 0.016 \ \text{g mL}^{-1}$; Connelly et al. 2014).

The uptake rate of each N source by nanoplankton ($UR_{s.Nano}$) was calculated using Eq. 9:

$$UR_{s.Nano} = UR_{<20.s} - UR_{<3.s} \quad (9)$$

where $UR_{<20.s}$ and $UR_{<3.s}$ represent the bulk uptake rate of each N by microbial communities of the $<20 \ \mu\text{m}$ and $<3 \ \mu\text{m}$ cell size, respectively.

The uptake rate of each N source by picoplankton taxa ($UR_{s.PicoT}$) at site I1 was calculated using Eqs. 10–13. The total ^{15}N contents (TNC) of pico-eukaryotes (Euk) and archaea (Arch) in the $<3 \ \mu\text{m}$ cell-size microbial communities ($TNC_{<3.s.Euk/Arch}$) were calculated using Eq. 10; those of heterotrophic bacteria (HB) and *Prochlorococcus* (Pro) ($TNC_{<3.s.HB/Pro}$) were calculated using Eq. 11:

$$TNC_{<3.s.Euk/Arch} = A_{<3.s.Euk/Arch} \times P_{<3.s.Euk/Arch} \times NC_{<3.s.Euk/Arch} \quad (10)$$

$$TNC_{<3.s.HB/Pro} = A_{<3.s.Bac} \times P_{<3.s.Bac} \times ra_{<3.s.HB/Pro} \times NC_{<3.s.HB/Pro} \quad (11)$$

where <3 represents microbial communities of the $<3 \ \mu\text{m}$ cell size, $A_{<3.s.T}$ is the total abundance of taxon T (Euk, Arch, or Bac) (Supporting Information Table S2), $P_{<3.s.T}$ is from Eq. 8, and $ra_{<3.s.HB/Pro}$ is the relative abundance of heterotrophic bacteria or *Prochlorococcus* in an actively N-incorporating prokaryote community (determined by 16S rRNA genes sequencing of ^{15}N-DNA; *Synechococcus* was extremely low-abundant); NC is the cell N content of heterotrophic prokaryotes, *Prochlorococcus*, and pico-eukaryotes, which was estimated as $1.5 \ \text{fg N cell}^{-1}$, $6.6 \ \text{fg N cell}^{-1}$, and $28 \ \text{fg N cell}^{-1}$, respectively, according to their average cell carbon content and C/N molar ratio in open oceans (Supporting Information Table S3).

The relative ^{15}N content of picoplankton taxa (PicoT) in the $<3 \ \mu\text{m}$ cell-size microbial community ($RNC_{<3.s.picoT}$) was calculated using Eq. 12 and the uptake rate of each N by PicoT ($UR_{s.PicoT}$) was calculated using Eq. 13:

$$RNC_{<3.s.picoT} = \frac{TNC_{<3.s.PicoT}}{TNC_{<3.s.HB} + TNC_{<3.s.Pro} + TNC_{<3.s.Arch} + TNC_{<3.s.Euk}} \quad (12)$$

$$UR_{s.PicoT} = UR_{<3.s} \cdot RNC_{<3.s.PicoT} \quad (13)$$

where PicoT represents HB, Pro, Arch, or Euk.

The uptake rate of each N source by picoplankton taxa at site SEATS was calculated based on Eqs. 10–13 using the data from microbial communities of the $<20 \ \mu\text{m}$ cell size. This is because the uptakes of N sources between the $<20 \ \mu\text{m}$ and $<3 \ \mu\text{m}$ microbial communities were approximately equal, suggesting that nanoplankton played a negligible role for N uptake at this basin site. So, given the $<20 \ \mu\text{m}$ microbial communities could be more intact than the $<3 \ \mu\text{m}$ microbial communities, we used the data from the $<20 \ \mu\text{m}$ microbial communities to accurately compare the uptake rate of N by heterotrophic and autotrophic picoplankton.

The contribution of each population to bulk uptake of each N substrate ($C_{s.PicoT}$) was calculated using Eq. 14; the

contribution of each N to total N (sum of four N sources) uptake by each taxon ($C_{PicoT.s}$) was calculated using Eq. 15

$$C_{s.PicoT} = \frac{UR_{s.PicoT}}{UR_{<20.s}} \times 100\% \qquad (14)$$

$$C_{PicoT.s} = \frac{UR_{s.PicoT}}{UR_{NH_4^+.PicoT} + UR_{urea.PicoT} + UR_{NO_3^-.PicoT} + UR_{NO_2^-.PicoT}} \\ \times 100\%$$

$$(15)$$

Model simulations

Simulations of marine ecosystems and biogeochemical cycles were conducted using the Community Earth System Model 1.0. The biogeochemical/ecosystem model ran in the ocean physics component. The resolution chosen was roughly 1° horizontally and 60 vertical levels, with 10 m thickness of each vertical level in the upper 150 m. The initial distributions of nutrients, inorganic carbon, and alkalinity were based on the World Ocean Atlas database (Garcia et al. 2006) and the GLODAP database (Key et al. 2004). After spin-up under preindustrial conditions, the model took repeating atmospheric forcing from the National Center for Environmental Prediction/National Center for Atmospheric Research meteorological reanalysis climatology (Large and Yeager 2008), while atmospheric CO_2 increased from 278 ppm to the present-day level.

The biogeochemical/ecosystem model used here includes three phytoplankton functional groups (diatoms, diazotrophs, and small phytoplankton), one zooplankton group and biogeochemical cycling of multiple growth-limiting nutrients (N, phosphorus, silicon, and iron) (Moore et al. 2004). The light, nutrient, and temperature dependencies of phytoplankton growth rates were calculated. Phytoplankton growth rates decrease under nutrient stress according to Michaelis-Menten nutrient uptake kinetics. Biogeochemical/ecosystem model simulates the uptake of NO_3^- and NH_4^+ by various phytoplankton groups, as well as the N_2 fixation by diazotrophs that contribute new production into the system. This allows us to calculate carbon fixation supported by specific N sources using the Redfield C/N ratio.

We consider production supported by NO_3^- and N_2 fixation as the simulated new production. The total production is the sum of new production and production supported by NH_4^+. Due to limited computational resources, we calculated the corrected new production and *f*-ratio using an offline model based on simulated results from 2005 to 2009. Here, we considered the relative contribution of heterotrophic prokaryotic assimilation to both NO_3^- and NH_4^+ uptake within the euphotic zone of oligotrophic open basins, which is defined by greater than 1000 m water depth and low surface NO_3^- concentrations ($< 1\ \mu m$). Since NO_3^- concentrations generally start to increase vertically as PAR drops to 1% level, we incorporated the correction parameters of the 20% PAR depth and the 1% PAR depth to simulated new production in waters where

the NO_3^- concentrations are $\leq 1\ \mu mol\ L^{-1}$ and $> 1\ \mu mol\ L^{-1}$, respectively. Correction parameters were listed in Supporting Information Table S4. The correction was applied to areas between 45°N and 45°S only. We integrated corrected new production and total production over the upper 150 m, where biological activities were simulated explicitly in biogeochemical/ecosystem model. The corrected *f*-ratio was calculated by the following equation:

$$f\text{-ratio} = \frac{PP\_NO_{3\ correct}^- + PP\_N_{fix}}{PP\_NO_{3\ correct}^- + PP\_NH_{4\ correct}^+ + PP\_N_{fix}} \qquad (16)$$

where $PP\_NO_{3correct}^-$ and $PP\_NH_{4\ correct}^+$ represent the corrected production supported by NO_3^- and NH_4^+, respectively, using parameters from incubation experiments presented in this study and PP_N_{fix} represents the production supported by N_2 fixation. Note that the uptake of organic N by phytoplankton was not simulated in the present model version, and was left out from all calculations. We acknowledge the remaining caveat; however, further laboratory and field observations are needed to provide key information for model developments and more accurate simulations.

Statistics

For all comparisons between two variables, we used the nonparametric Wilcoxon rank-sum tests because a normal distribution of the individual data sets was not always met.

Results

Bulk potential uptake rates of N sources by the microbial community

Nitrate was depleted at the 20% PAR depth and the nitracline was around the 1% PAR depth; the primary NO_2^- maximum was at the 1% PAR depth at both sites I1 and SEATS. In contrast, regenerated N substrate (NH_4^+ and urea) concentrations were higher at a depth of 20% PAR than at 1% PAR (Fig. 1b,e). The deep chlorophyll maximum was at 65 m and 75 m water depth at I1 and SEATS, respectively, which was located above the 1% PAR depth in both sites (Fig. 1a,d). There was a higher abundance of pico-/nano-sized eukaryotes and *Synechococcus* at I1 (Wilcoxon rank-sum test, $p < 0.05$), whereas *Prochlorococcus* showed relatively higher abundance at SEATS ($p < 0.05$ in the upper 100 m; Fig. 1c,f).

The N uptake rates by either the $< 20\ \mu m$ or $< 3\ \mu m$ fraction of the microbial community were distinctly higher at I1 than at SEATS for both PAR depths ($p < 0.01$; Fig. 2a,b; Supporting Information Table S5). The uptake rate of each N source by the $< 20\ \mu m$ fraction was significantly higher than the $< 3\ \mu m$ fraction at I1 ($p < 0.05$; Fig. 2a) but, at SEATS, the uptake was similar for the two size communities (Fig. 2b). This suggested that there were more abundant nanoplankton (3–20 μm) at I1, but they were almost negligible at SEATS with almost all uptake of N species by picoplankton. The bulk uptake rates of
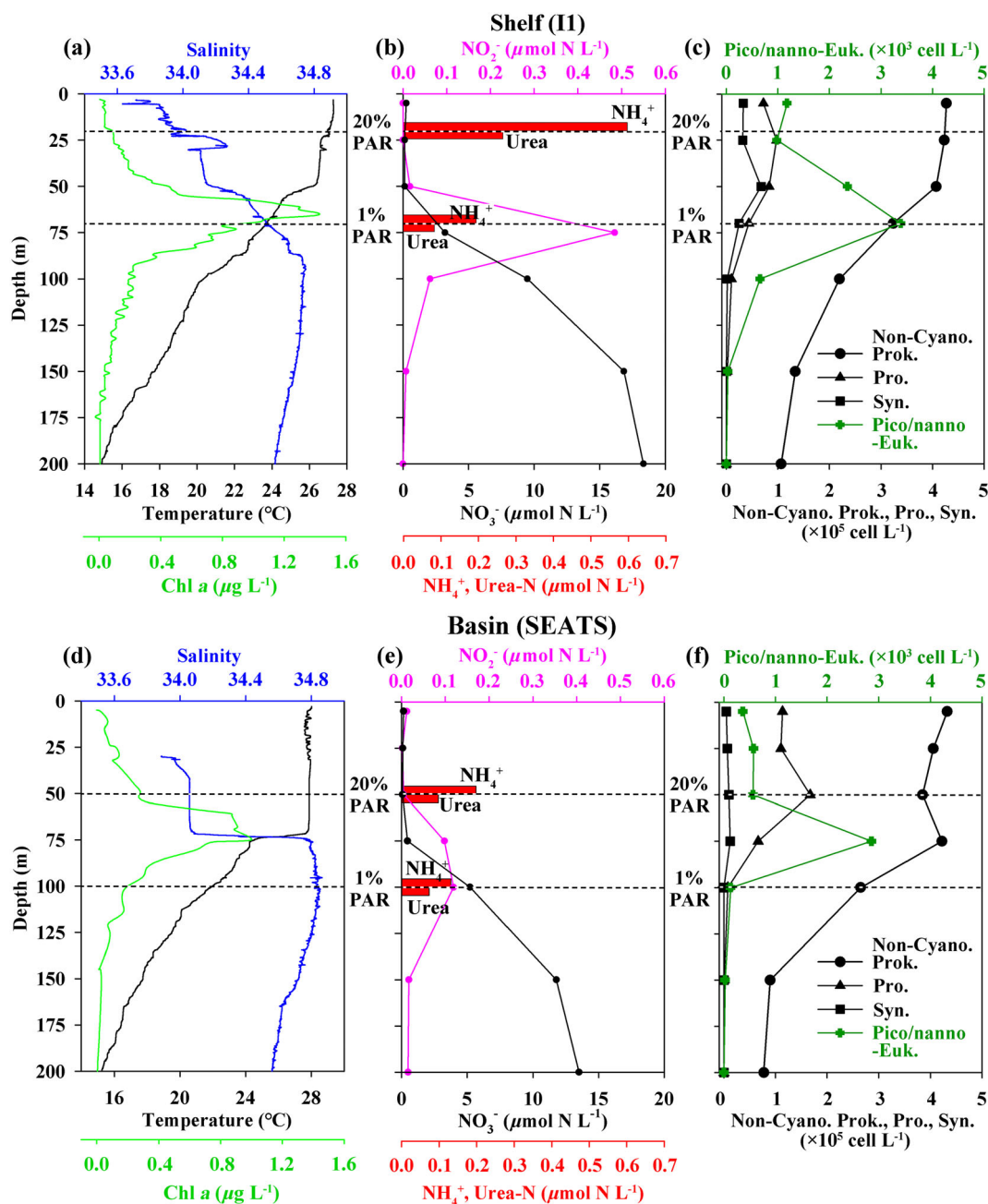
Fig 1. Biogeochemical parameters at the South China Sea (**a–c**) shelf site I1 and (**d–f**) open basin site SEATS. (**a, d**) Water depth profiles of temperature, salinity, and Chl *a* concentration. (**b, e**) Depth profiles of ammonium (NH_4^+), nitrate (NO_3^-), nitrite (NO_2^-), and urea concentrations. (**c, f**) Depth profiles of abundances of *Prochlorococcus* (Pro.), *Synechococcus* (Syn.), eukaryotes (Euk.), and noncyanobacterial prokaryotes (Non-Cyano. Prok.).

regenerated N (NH_4^+ and urea) were higher than NO_3^- and NO_2^- in general ($p < 0.05$), except for the relatively higher NO_3^- uptake by the $< 20 \mu m$ fraction at the 1% PAR depth of I1 (Fig. 2a; Supporting Information Table S5).

Uptake of N sources by the eukaryotic, bacterial, and archaeal populations

The normalized distribution of bacterial (hereafter defined as combined heterotrophic bacteria and cyanobacteria) 16S rRNA, eukaryotic 18S rRNA, and archaeal 16S rRNA and *amo*A gene copies in the CsCl density gradient (scaled between 0 and 1 along the gradient) were analyzed to estimate the degree of ^{15}N labeling of these DNA (Supporting Information Figs. S2, S3), which is an index of N uptake activity. The eukaryotic, bacterial, and archaeal populations assimilated more N at I1 than at SEATS ($p < 0.01$; Fig. 2c,d). Notably, there was no significant difference between the eukaryotic and bacterial N uptakes, and their uptakes were generally higher than
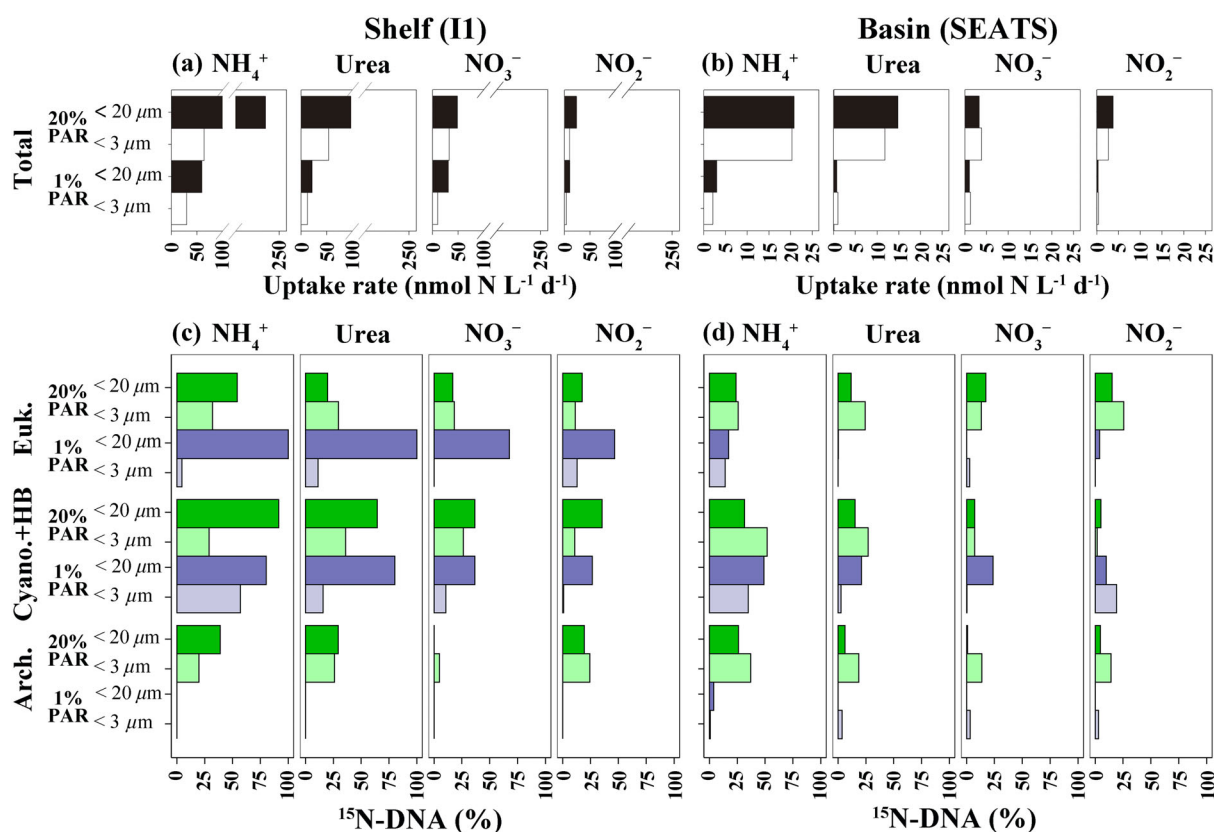
Fig 2. (**a**, **b**) Bulk uptake rate of ammonium (NH_4^+), nitrate (NO_3^-), nitrite (NO_2^-), and urea by the microbial community and (**c**, **d**) percentage of ^{15}N-labeled DNA of bacterial (including cyanobacteria and heterotrophic bacteria, Cyano.+HB), eukaryotic (Euk.), and archaeal (Arch.) DNA at the South China Sea (**a**, **c**) shelf site I1 and (**b**, **d**) open basin site SEATS.

archaeal uptake in all samples ($p < 0.01$). The eukaryotes assimilated more N at the 20% PAR depths than at the 1% PAR depths at both sites ($p < 0.01$), except for the relatively higher uptakes in the $< 20\ \mu m$ communities at 1% PAR of I1 ($p < 0.05$; Fig. 2c). The bacterial N uptake showed no significant difference between the two depths; the archaeal N uptake at the 20% PAR was distinctly higher than at the 1% PAR ($p < 0.01$; Fig. 2c,d). In general, the eukaryotes, bacteria, and archaea had similar uptakes between NH_4^+ and urea, between NO_3^- and NO_2^- at I1 and significantly higher uptakes of NH_4^+ and urea than of NO_3^- and NO_2^-, respectively ($p < 0.05$; Fig. 2c). At SEATS, however, the three populations had higher uptakes of NH_4^+ than of urea, NO_3^-, and NO_2^- ($p < 0.01$; Fig. 2d).

In addition, archaeal *amo*A genes were undetectable in all CsCl gradient fractions from the 20% PAR depths at the two sites (Supporting Information Figs. S2a,b, S3a,b). However, in the samples from the 1% PAR depths (Supporting Information Figs. S2c,d, S3c,d), archaeal *amo*A gene and 16S rRNA gene abundances peaked in the light density fraction, indicating that there were ammonia-oxidizing archaea at the 1% PAR depth and they incorporate extremely minor ^{15}N sources into their DNA.

Actively N-incorporating prokaryotic populations

The ^{15}N (heavy) and ^{14}N (light) DNA sequence analyses revealed a significant difference in bacterial and archaeal community composition between the 20% and 1% PAR depths at both I1 and SEATS (analysis of similarity test, $p < 0.01$; Supporting Information Fig. S4). The bacterial heavy and light fractions from the same depth and size clustered separately when the N uptake was high (e.g., at 20% PAR depths or for $< 20\ \mu m$ communities), and clustered together when the uptake was relatively low (e.g., at 1% PAR depths or for $< 3\ \mu m$ communities).

Phylogenetic analysis indicated that *Prochlorococcus* was clearly dominant among the N-incorporating (^{15}N-DNA) populations (Fig. 3). It actively incorporated N sources, especially at the 20% PAR depth, and was relatively more abundant at SEATS than at I1 ($p < 0.05$). The main competitors of N incorporation with *Prochlorococcus* at the 20% PAR depth were members of *Rhodobacteraceae*, *Erythrobacter*, *Henriciella* (*Hyphomonas*), and *Alteromonas* at I1 and diverse low-abundant taxa of Flavobacteria, α-Proteobacteria, γ-Proteobacteria, and Actinobacteria at SEATS (Fig. 3). The N sources at the 1% PAR depth were incorporated by members of

Rhodobacteraceae, *Erythrobacter*, and *Alteromonas* at both sites; *Pseudomonas*, *Alcanivorax*, and *Marinobacter* at I1; and *Oleiphilus* and *Acidimicrobineae* (Actinobacteria) at SEATS. In addition, there were many very low-abundant N-incorporating taxa, such as a few members from SAR11, SAR86, and SAR406, at the two sites (Fig. 3). Bacterial populations that did not incorporate N (^{14}N-DNA; Supporting Information Fig. S5) at the two sites mainly included SAR11, some unclassified OTUs
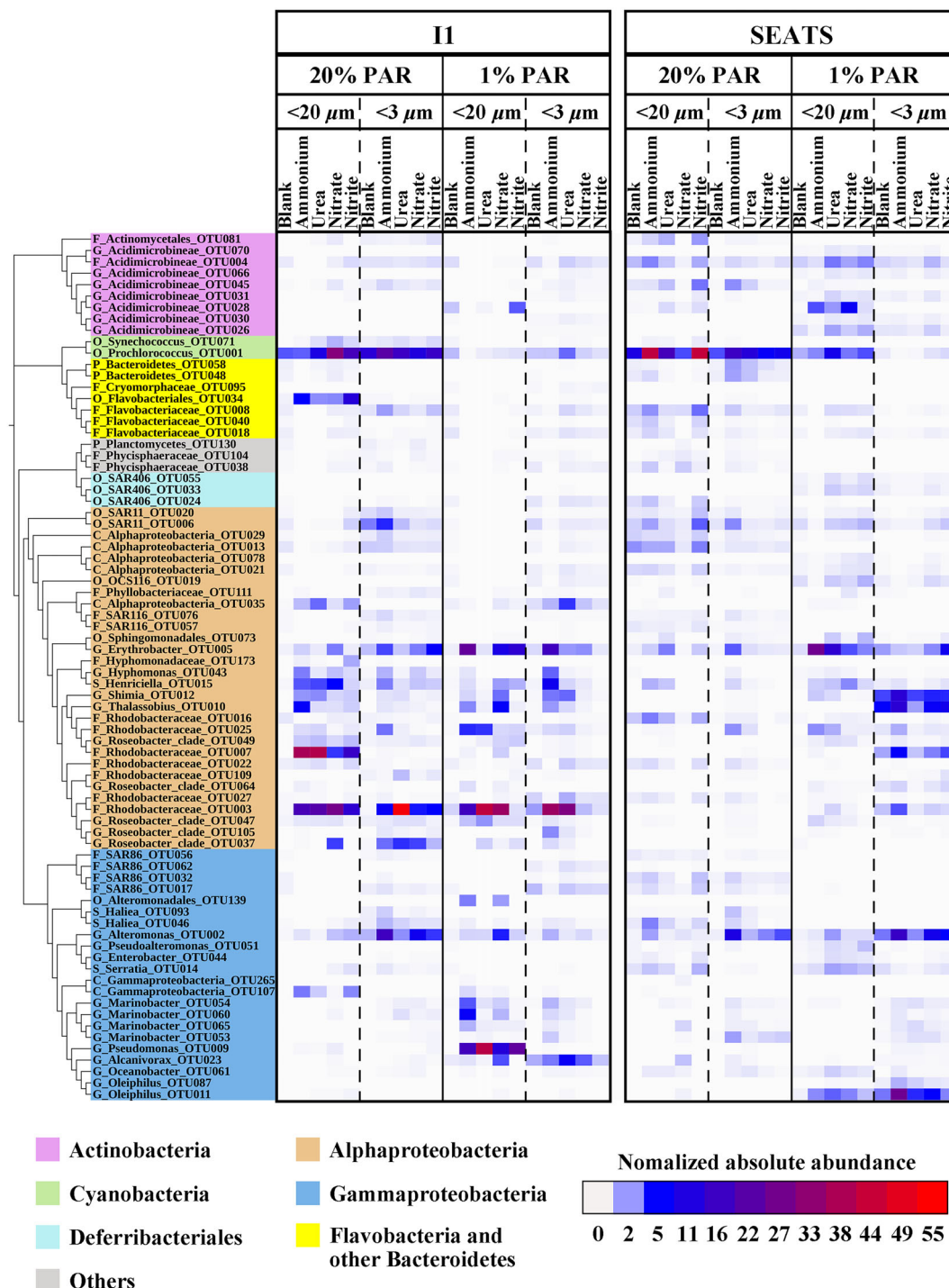

Fig 3. Phylogenetic tree of bacterial OTU sequences with relative abundance > 1% of total 16S rRNA gene sequences (*n* > 62 sequences) in any one of the representative heavy fractions. The normalized abundances (*see* "Materials and methods" section) are shown as heat maps to the right of the phylogenetic tree; they are comparable only within each incubation sample (one column). The figure was produced from the Interactive Tree Of Life (iTOL, http://itol.embl.de/). C, class; F, family; G, genus; K, kingdom; O, order; P, phylum

that clustered together with SAR11, SAR86 (γ-Proteobacteria), and SAR406, as well as diverse members from Flavobacteria and Actinobacteria, although they also included members of *Rhodobacteraceae*, *Erythrobacter*, *Alteromonas*, and *Oleiphilus*. The active N-incorporating archaeal populations were mainly Euryarchaeota MG II and III and some unclassified archaeal OTUs at the 20% PAR depth at both sites. Thaumarchaeota MG I dominated the archaeal communities at the 1% PAR depth and absolutely concentrated in the (ultra)light fractions with extremely minor incorporation of ^{15}N (Fig. 4).

Taxon-specific N assimilation

By combining bulk uptake rates of N and percentages of taxon-specific ^{15}N-DNA, we were able to estimate taxon/population-specific N assimilation further (Supporting Information Table S6). Shelf site I1 is a relatively eutrophic environment, with more abundant nanoplankton than was found in the open basin site SEATS, which led to higher N uptake by nanoplankton (Fig. 5a; ~ 61% and ~ 54% of total N [sum of four N sources] uptake at the 20% and 1% PAR depths, respectively) in competition with cyanobacteria (mainly

Prochlorococcus in this study; only ~ 20% and ~ 4%). At I1, total heterotrophic prokaryotes were inferred to contribute ~ 17% and ~ 41% of total N uptake at the 20% PAR and 1% PAR depths, respectively (Fig. 5a). Heterotrophic archaea contributed extremely minor levels of N uptake at both I1 and SEATS owing to their low abundance (Supporting Information Tables S2, S6). The picoplankton—mainly *Prochlorococcus*, heterotrophic bacteria, and pico-eukaryotes—dominated the total N uptake at SEATS (Fig. 5b). *Prochlorococcus* contributed ~ 54% and ~ 17% of total N uptake at the 20% and 1% PAR depths, respectively, whereas heterotrophic prokaryotes contributed ~ 19% and ~ 55%, respectively, at the two depths (Fig. 5b). Pico-eukaryotes contributed ~ 27% of total N uptake at both depths at SEATS, while they only contributed < 2% of total N uptake at I1. Autotrophic nitrifiers, that is, ammonium-oxidizing archaea and bacteria as well as nitrite-oxidizing bacteria, were not technically discriminated from these data because they were extremely low abundant and contributed negligible N uptake at both I1 and SEATS.

Among the four N sources, almost all of the populations assimilated more regenerated N source (mostly NH_4^+; Supporting
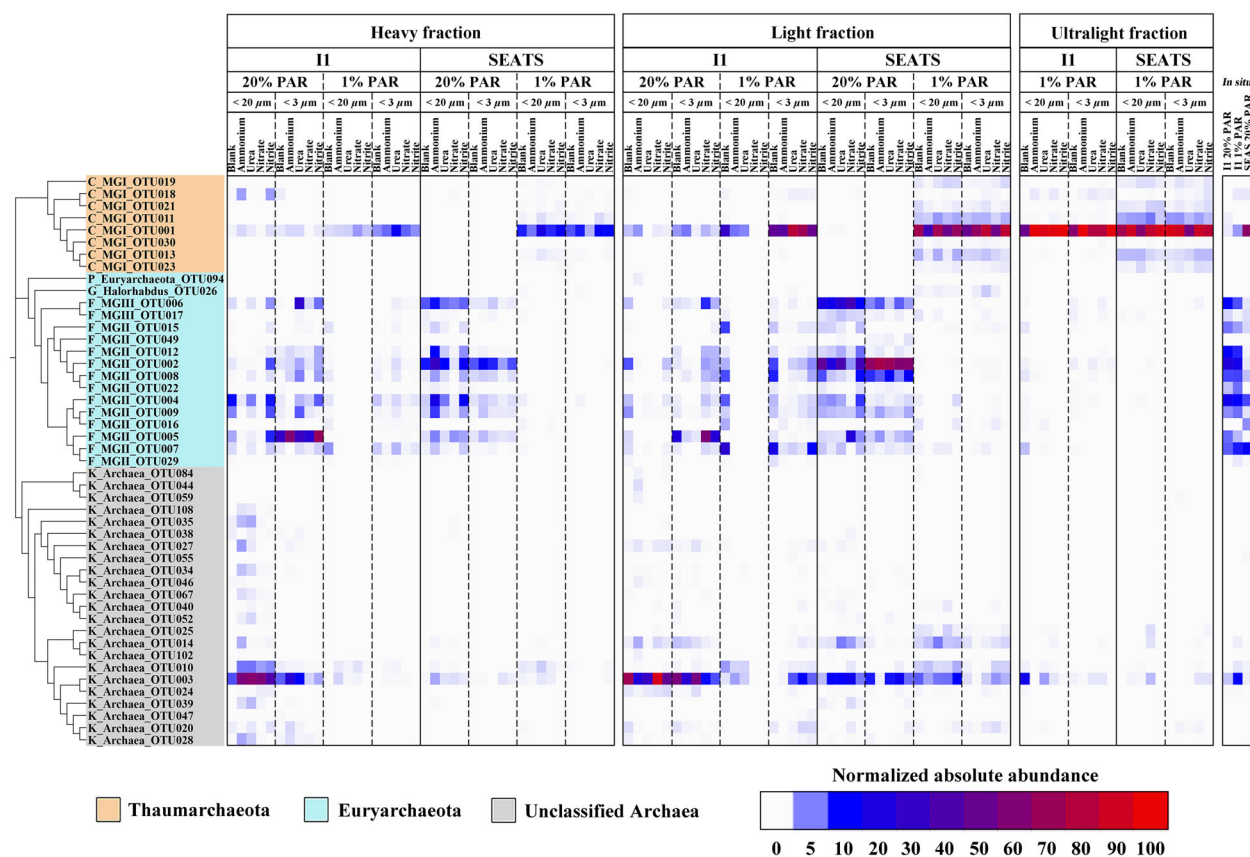

Fig 4. Phylogenetic tree of archaeal OTU sequences with relative abundance > 1% of total 16S rRNA gene sequences (more than six sequences) in any one of the representative heavy, light, ultralight fractions, and in situ samples. The normalized abundances are shown as heat maps to the right of the phylogenetic tree; they are comparable only within each incubation sample (including three columns). The figure was produced from the Interactive Tree Of Life (iTOL, http://itol.embl.de/). C, class; F, family; G, genus; K, kingdom; P, phylum

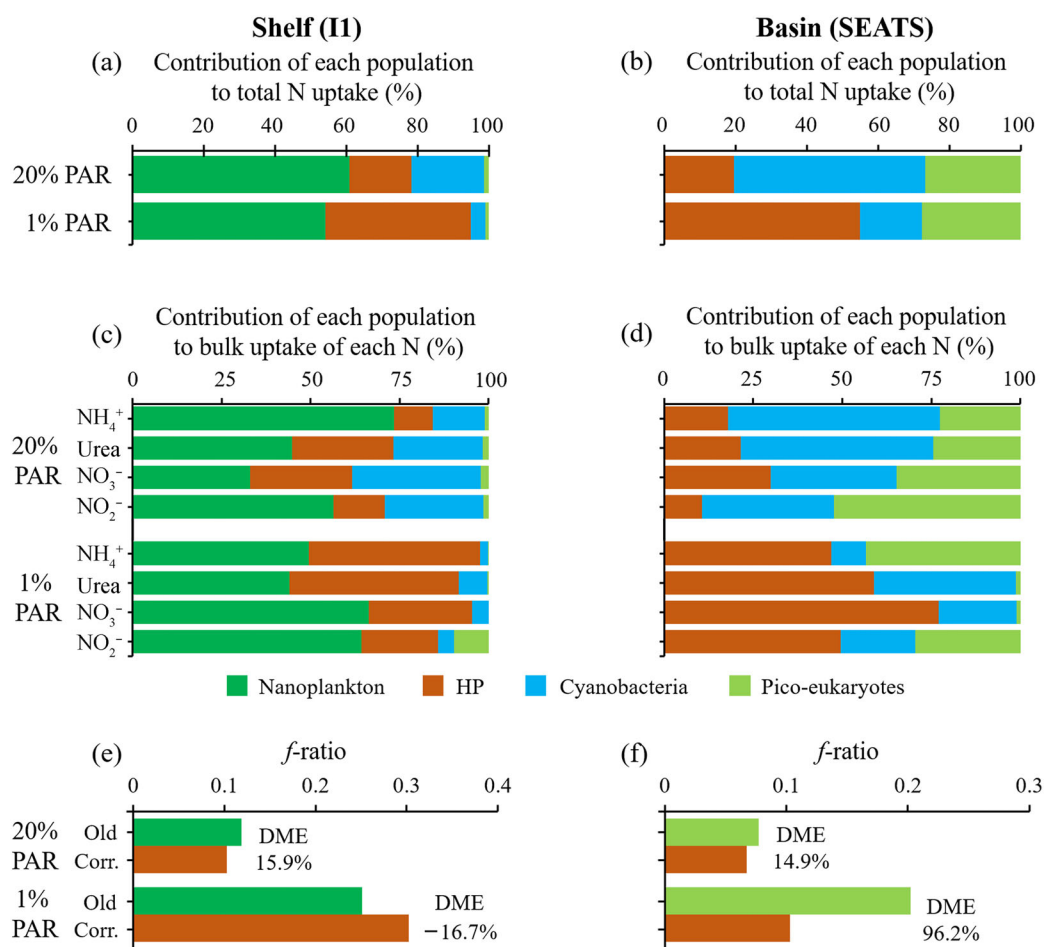**Shelf (I1)**   **Basin (SEATS)**

Fig 5. (**a**, **b**) Contribution of each population (nanoplankton, heterotrophic prokaryotes [HP], cyanobacteria, and pico-eukaryotes) to total nitrogen (N; sum of ammonium [NH_4^+], nitrate [NO_3^-], nitrite [NO_2^-], and urea) uptake by the microbial community, (**c**, **d**) contribution of each population to bulk uptake of each N, as well as (**e**, **f**) *f*-ratio (= NO_3^- uptake/total N uptake) and the degree of misestimation (DME% = [old − corrected]/corrected) of *f*-ratio caused by heterotrophic prokaryotic N uptake at the South China Sea (**a**, **c**, **e**) shelf site I1 and (**b**, **d**, **f**) open basin site SEATS. Corr., corrected.

Information Fig. S6 and Table S6). Notably, however, heterotrophic prokaryotes made a relatively higher contribution (~ 29% at I1 and 30% at SEATS; Supporting Information Table S4) to bulk uptake of NO_3^- by the total microbial community than of NH_4^+ and urea at the 20% PAR depths, where abundant autotrophic plankton contributed more to bulk uptake of regenerated N (Fig. 5c,d). The pattern was the opposite at the 1% PAR depth of I1, where regenerated N concentrations were low and abundant nanoplankton contributed more to bulk uptake of NO_3^- (Fig. 5c). At the 1% PAR depth of SEATS, there were only a few pico-sized autotrophic plankton, and thus heterotrophic prokaryotes contributed significantly to bulk uptakes of all four N sources (47–77%), and especially of NO_3^- (Fig. 5d; Supporting Information Table S4).

Discussion

To obtain sufficient ^{15}N-labeled DNA from open oceans, we carried out a large volume (10 L) of incubation with the

addition of relatively high concentration of substrate (Supporting Information Table S7) and relatively long-time incubation (36 h) under in situ temperature and light condition. In such incubation systems, we sought to maintain the similar activities of microbial populations to those in the environment as much as possible. Our data showed that the abundances of *Prochlorococcus*, *Synechococcus*, and heterotrophic prokaryotes, as well as pico-eukaryotes, maintain generally stable during incubations (Supporting Information Tables S8, S9); the bulk potential uptake rates of each N source were within the range of the inferred rates reported previously in the Atlantic and Pacific Oceans (Supporting Information Table S10); and the assimilated concentration of each N source during the incubations was lower than the in situ concentration (Supporting Information Table S7), except that the assimilated NO_2^- concentration was higher than the ultralow in situ concentration at the 20% PAR depth of I1. These data indicated that the potential N uptake rates by the microbial communities were still limited probably due to the low availability

of other nutrients, like iron for phytoplankton and organic matter for heterotrophic bacteria. None of the above four populations decayed or bloomed during the incubations. Thus, we can compare N assimilation among these populations. Our experimental scenario probably reflects the potential competition between heterotrophic prokaryotes and autotrophic picoplankton for episodically imported N sources, for example, during the occurrence of upwelling in open oceans.

To assess regenerated sources of N during the incubations and separate the direct inorganic N assimilation and indirect uptake of labeled organic materials, we measured concentration and N isotopic composition of DON in the incubation systems with added $^{15}NH_4^+$. The ^{15}N-labeled DON released by microbial communities accounted for only an extremely minor fraction of the total DON pool (0.08–0.85%) and dissolved ^{15}N pool (0.33–3.63%) (Supporting Information Table S11). The ^{15}N enrichment in the DON pool was likely underestimated given DON could be broken down to NH_4^+ during the pretreatment process (Bronk and Ward 2000). While the possibility of cross-feeding cannot be completely precluded, its effects may be limited and ^{15}N-DNA was mainly derived from the inorganic N assimilation. This can also be evidenced by the significant differences between the N-incorporating and N-unincorporating bacterial communities when the N uptake rates were high (Supporting Information Fig. S4). In addition, highly correlated linear regressions between the particulate ^{15}N production and incubation time (Supporting Information Fig. S7) suggest that the isotope dilution effect, community changes, and cross-feeding effects were minimal during the incubations. The negligible isotope dilution was due to the large isotope additions used. Nevertheless, incubation as short as possible is encouraged to avoid any potential cross-feeding effect.

Overall, the potential bulk uptake rates by the microbial communities and population-specific N assimilation indicated that NH_4^+ was the most preferred N source, followed by urea, NO_3^-, and NO_2^-. This is generally consistent with the percentages of ^{15}N-DNA of total eukaryotic, bacterial, and archaeal DNA, although each OTU varied in assimilation capability of the four N sources. Ammonium can be utilized directly by metabolic pathways in cells; however, NO_3^- needs first to be reduced to NH_4^+ before utilization, which requires at least five nicotinamide adenine dinucleotides and thus consumes more energy than NH_4^+ assimilation (Kirchman 2002;). Urea is transported across the cell membrane via adenosine triphosphate-binding cassette transporters that use energy from adenosine triphosphate and then split into NH_4^+ and CO_2 by urease (Solomon et al. 2010). In theory, the energetic cost of NO_2^- assimilation is lower than NO_3^- assimilation, but the accumulation of NO_2^- inside cells is toxic (Moir and Wood 2001). Though the incorporation of reduced N (e.g., NH_4^+) is more energy-efficient than oxidized N, ammonium is not necessarily the constituent most assimilated in the environment

because it can be more limiting in the environment than in the experiment (Aldunate et al. 2020).

The active N-incorporating bacteria in the South China Sea were mainly Cyanobacteria, α-Proteobacteria, and γ-Proteobacteria. Our results found that *Prochlorococcus* (OTU001) incorporate NH_4^+, urea, NO_3^-, and NO_2^- strongly to weakly, similar to bulk N uptake rates. The uptake rates of flow-cytometer-sorted Sargasso Sea *Prochlorococcus* revealed that it assimilated more urea than the other three DIN components (Casey et al. 2007). *Prochlorococcus* commonly relies on recycled N in the euphotic zone (Moore 2002; Fawcett et al. 2011). The discovery of a genomic island containing NO_3^- and NO_2^- assimilation genes in the metagenome of *Prochlorococcus* from marine surface waters (Martiny et al. 2009), and strains able to grow on NO_3^- as the sole source of N (Berube et al. 2015), however, suggested that oxidized N may be a significant source of N in the natural environment under certain nutrient conditions. For instance, *Prochlorococcus* was found, based on natural abundance of isotopes in cells, to use NO_2^- as the dominant N source in the oxygen-deficient zones of the Eastern Tropical North and South Pacific where NH_4^+ was limiting (Aldunate et al. 2020).

Notably, highly diverse taxa of heterotrophic bacteria incorporated N sources. Among them, the dominant members of *Rhodobacteraceae*, *Erythrobacter*, and *Alteromonas* incorporated each N source when it alone was added, suggesting that these taxa have the capability to adapt to varying nutrient conditions and compete for N with other populations (Goddard and Bradford 2003; Berthelot et al. 2019). Generally, the N-incorporating taxa were limited in specific communities from different sites, depths, and size fractions. Previous SIP studies also showed various N-incorporating taxa in different environments; for example, NH_4^+ assimilation by Flavobacteria and *Rhodobacteraceae* in the Southern California Bight (Morando and Capone 2018), NH_4^+ and NO_3^- incorporation by *Thalassobacter* (*Rhodobacteraceae*) and *Alteromonadales* on the West Florida Shelf (Wawrik et al. 2012), urea uptake by β-Proteobacteria, *Firmicutes*, SAR11, and SAR324 offshore of Barrow in the Arctic (Connelly et al. 2014), as well as NO_3^- assimilation by a specific subclade of SAR11 in the Big Fisherman's Cove off Catalina Island, U.S.A. (Morando and Capone 2016). This suggests that a wide spectrum of heterotrophic bacteria could incorporate DIN and urea and potentially compete with cyanobacteria in a wide range of environments, especially in the scenario of episodic import of N sources. In the present study, SAR11 OTUs (~ 10% of the total for the in situ communities) incorporated minor ^{15}N and were relatively more enriched in the N-unincorporating assemblages. These results contrast with Widner et al. (2018) who found, based on metagenomic and metatranscriptomic analyses, that a fraction of SAR11 and *Nitrospina* have the potential and activity to use urea in the Eastern Tropical North Pacific oxygen-deficient zone. However, due to a very low in situ abundance (only < 0.6% of relative abundance at the 1%

PAR depths of both sites) in this study, *Nitrospina* OTUs were not retrieved from the ^{15}N-DNA except for $<0.2\%$ of relative abundance at the 1% PAR depth of SEATS.

The bulk potential uptake rates of N sources by size-fractionated communities suggest that there were more abundant nanoplankton at I1. Considering potential nanoflagellate predation on prokaryotes was removed in the $<3\ \mu m$ microbial community, the abundance of prokaryotes in the $<3\ \mu m$ communities should have been higher than that in the $<20\ \mu m$ communities. However, the experimental result was contrary. Moreover, the percentages of bacterial ^{15}N-DNA decreased significantly with the removal of nano-sized particles at I1, and this decrease resulted from heterotrophic bacteria, as revealed by the phylogenetic analysis. This is consistent with higher abundances of *Prochlorococcus* sequences retrieved from ^{15}N-DNA than of each heterotrophic bacterial taxon at the 20% PAR depth of SEATS, where nanoplankton was negligible. This suggests that heterotrophic bacteria might benefit from nanoplankton (and other particles) competing for N sources with *Prochlorococcus*, because of the stimulated DIN uptake by available labile organic carbon (Kirchman et al. 1990; Jacquet et al. 2002; Bradley et al. 2010). Overall, the actively N-incorporating taxa at the 1% PAR depth of both sites were composed of abundant heterotrophic bacteria that outcompeted *Prochlorococcus* for DIN and urea uptake during the incubations.

Archaeal abundance and N-incorporating activity were much lower than bacteria within the euphotic zone. The vast majority of the archaeal N incorporation was detected at the 20% PAR depth, although archaea were more abundant at the 1% PAR depth (Karner et al. 2001). Euryarchaeota MG II, which are usually the most abundant heterotrophic archaeal taxon in ocean surface water (Zhang et al. 2015), were main N-incorporators at the 20% PAR depth. Thaumarchaeota MG I, which are ammonia-oxidizing chemolithoautotrophs, incorporated minor N sources at the 1% PAR depth. However, they could compete for ammonium by ammonia oxidization (Wan et al. 2018), which could not be determined by SIP. Similarly, they also could compete for urea by oxidizing urea-derived N (Qin et al. 2014; Bayer et al. 2016). Notably, Thaumarchaeota was found, using DNA-SIP, to assimilate carbon directly from urea by the reverse ornithine cycle in the mesopelagic and bathypelagic North Atlantic (Seyler et al. 2018).

Significant N uptake by heterotrophic prokaryotes would result in overestimates of the assimilation of both new and regenerated N by autotrophic plankton and bias the *f*-ratio. Although 0.3 μm pore size of GF filters used in this study is smaller than the nominal sizes (0.7 μm; the effective pore size must be $<0.5\ \mu m$; Morel et al. 1993; Chavez et al. 1995) of GF/F filters that are usually used to measure the N uptake of phytoplankton, the potential competition for N substrates between heterotrophic prokaryotes and autotrophic picoplankton and the impacts of heterotrophic N uptake on these estimates are noticeable because GF/F filters can retain a significant portion of the prokaryotes (Chavez et al. 1995;

Gasol and Moran 1999). Overestimate or underestimate of the *f*-ratio depends on the higher or lower relative contribution of heterotrophic prokaryotes to bulk uptake of new N than regenerated N. For instance,

$$f\text{-ratio} = \frac{\text{UR\_NO}_3^-}{\text{UR\_NH}_4^+ + \text{UR\_NO}_3^-}, \tag{17}$$

and then the corrected *f*-ratio that excludes the N uptake by heterotrophic prokaryotes is calculated as

$$
\begin{aligned}
f\text{-ratio}_{\text{corr}} &= \frac{\text{UR\_NO}_3^- - \text{UR\_NO}_{3\,\text{HP}}^-}{\left(\text{UR\_NH}_4^+ - \text{UR\_NH}_{4\,\text{HP}}^+\right) + \left(\text{UR\_NO}_3^- - \text{UR\_NO}_{3\,\text{HP}}^-\right)} \\[2mm]
&= \frac{\text{UR\_NO}_3^-\left(1 - C_{\text{NO}_3^-.\text{HP}}\right)}{\text{UR\_NH}_4^+\left(1 - C_{\text{NH}_4^+.\text{HP}}\right) + \text{UR\_NO}_3^-\left(1 - C_{\text{NO}_3^-.\text{HP}}\right)} \\[2mm]
&= \frac{\text{UR\_NO}_3^-}{\text{UR\_NH}_4^+ \times \frac{1 - C_{\text{NH}_4^+.\text{HP}}}{1 - C_{\text{NO}_3^-.\text{HP}}} + \text{UR\_NO}_3^-}
\end{aligned}
$$

$$\tag{18}$$

where UR_NO_3 and UR_NH_4^+ represent the bulk uptake rate of NO_3^- and NH_4^+ by the total community, respectively; $\text{UR\_NO}_{3\text{HP}}$ and $\text{UR\_NH}_{4\,\text{HP}}^+$ represent the uptake rate of NO_3^- and NH_4^+ by heterotrophic prokaryotes, respectively; $C_{\text{NO}_3.\text{HP}}$ and $C_{\text{NH}_4^+.\text{HP}}$ represent the contribution of heterotrophic prokaryotes to bulk uptake of NO_3^- and NH_4^+, respectively. When heterotrophic prokaryotes make a higher contribution to bulk uptake of NO_3^- ($C_{\text{NO}_3.\text{HP}}$) than of NH_4^+ ($C_{\text{A.HP}}$), the value of $\frac{1 - C_{\text{NH}_4^+.\text{HP}}}{1 - C_{\text{NO}_3.\text{HP}}}$ is >1. Then, the denominator in Eq. 18 is higher than the denominator in Eq. 17 resulting in the lower $f-\text{ratio}_{\text{corr}}$ than *f*-ratio, that is, the *f*-ratio is overestimated. It is thus clear that the over- or underestimate of *f*-ratio depends on the contribution of heterotrophic prokaryotes to bulk uptake of NO_3^- vs. NH_4^+ by the total community $\left(\frac{1 - C_{\text{NH}_4^+.\text{HP}}}{1 - C_{\text{NO}_3.\text{HP}}}\right)$ (data shown in Fig. 5), and does not depend on the contribution of each N to the four N sources uptake by each taxon ($C_{\text{PicoT.s}}$) (data shown in Supporting Information Fig. S6).

Our study revealed that, despite more assimilation of regenerated N source than NO_3^-, heterotrophic prokaryotes made a relatively higher contribution to bulk uptake of NO_3^- by the total microbial community than of NH_4^+ and urea, and thus there was a tendency to overestimate ($\sim 16\%$ and $\sim 15\%$ in I1 and SEATS, respectively) the *f*-ratio (not including N_2 fixation) at the 20% PAR depths (Fig. 5e,f), where it is suggested that abundant autotrophic plankton are more competitive for regenerated N relative to new N. Similarly, there was a distinct overestimate ($\sim 96\%$) of the *f*-ratio at the 1% PAR of SEATS, where nanoplankton are negligible and a few pico-sized autotrophic plankton are assumed to be more competitive for energetically inexpensive reduced forms of N. Only at the 1% PAR
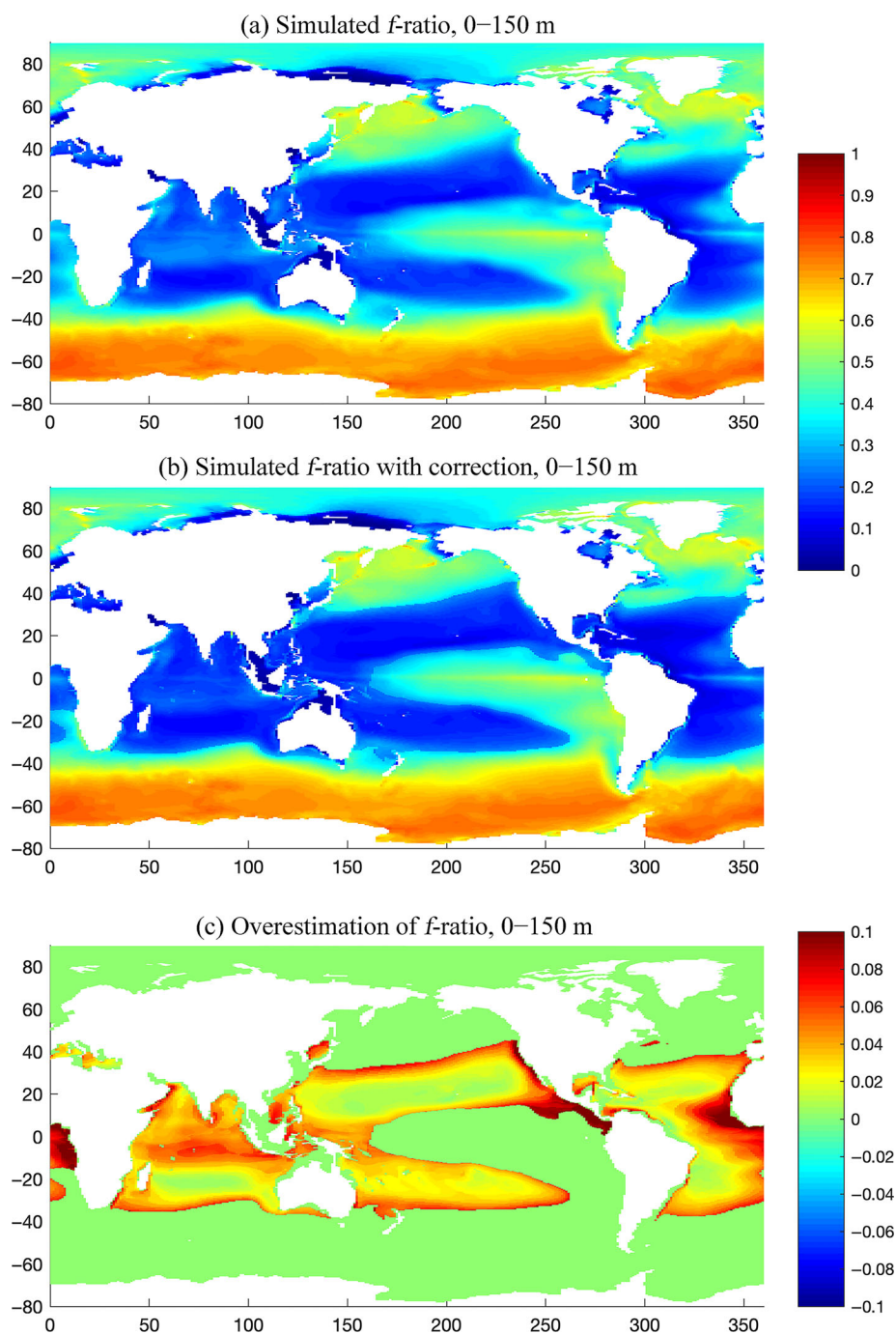
Fig 6. The simulated *f*-ratios (**a**) before and (**b**) after correction and (**c**) overestimation of *f*-ratios caused by heterotrophic prokaryotic assimilation of nitrate within the eutrophic zone (0–150 m) of the low and middle latitude oligotrophic open ocean during 2005–2009.

of I1 did heterotrophic prokaryotes have a higher relative contribution to bulk uptake of NH_4^+ and urea than of NO_3^-, and thus there was an underestimate (~ 17%) of the *f*-ratio (Fig. 5e) because of relatively higher uptake of NO_3^- by nanoplankton under low NH_4^+. The relatively higher contribution of heterotrophic prokaryotes to bulk uptake of NO_3^- has also been found in the oceanic sub-Arctic Pacific (Kirchman and

Wheeler 1998), the North Water of the Arctic Ocean (Fouilland et al. 2007), and the marginal ice zone of the Barents Sea (Allen et al. 2002). We speculated that, when autotrophic plankton (e.g., pico-sized) are more competitive for regenerated N in the high ambient NO_3^- concentrations and release the relatively low N content organic matter (Hopkinson and Vallino 2005), heterotrophic prokaryotes

may be forced to supplement N from NO_3^- for growth (Middelburg and Nieuwenhuize 2000).

Based on the above analyses of data from the relatively eutrophic shelf site (I1) and oligotrophic ocean site (SEATS), we find that phytoplankton community composition could regulate the contribution of heterotrophic prokaryotes to bulk uptake of NO_3^- vs. regenerated N. When eukaryotic phytoplankton are dominant in the relatively eutrophic waters, N is primarily taken up by phytoplankton; since different phytoplankton may be competitive for different N sources (either regenerated N or NO_3^-), the contribution of heterotrophic prokaryotes to bulk uptake of NO_3^- could be either higher or lower than regenerated N, resulting in either overestimate or underestimate of *f*-ratio. However, in the oligotrophic open ocean, *Prochlorococcus* (pico-sized and prokaryotic) may be dominant and relatively more competitive for regenerated N, which probably causes the relatively higher contribution of heterotrophic prokaryotes to bulk uptake of NO_3^-. We tried to extrapolate the parameters obtained from incubation experiments at SEATS to the oligotrophic open ocean ($>1000\,m$ depth, $<1\ \mu mol\,L^{-1}$ surface NO_3^- concentration, and between $45°N$ and $45°S$) where *Prochlorococcus* is widespread (Flombaum et al. 2013) to gain an insight of how heterotrophs influence the open oceanic *f*-ratio estimate. The global model simulated that the *f*-ratio (including N_2 fixation) would decrease ~18% with our observations-based correction in the low-latitude oligotrophic open ocean (Fig. 6).

Collectively, phylogenetically diverse heterotrophic prokaryotes had the capability to contribute a significant fraction of DIN and urea uptake, potentially competing with cyanobacteria in the oceanic euphotic zone. When nano-sized phytoplankton are negligible and cyanobacteria are dominant (e.g., in the low-latitude open ocean), heterotrophic prokaryotes may make a higher contribution to bulk uptake of NO_3^- relative to regenerated N, and thus there was a tendency to overestimate the *f*-ratio, especially in the scenario of episodic import of N sources (e.g., upwelling). This suggests a more prominent biogeochemical role of heterotrophic prokaryotes in these areas than hitherto assumed. This work highlights the importance of distinguishing the DIN and urea uptake by heterotrophic prokaryotes from that of autotrophic plankton—and particularly of cyanobacteria—in the open ocean to better understand oceanic new and regenerated production, and the stoichiometric relationship between carbon fixation and N substrate uptake in the ocean.

References

Aldunate, M., C. Henríquez-Castillo, Q. Ji, J. Lueders-Dumont, M. R. Mulholland, B. B. Ward, P. von Dassow, and O. Ulloa. 2020. Nitrogen assimilation in picocyanobacteria inhabiting the oxygen-deficient waters of the eastern tropical North and South Pacific. Limnol. Oceanogr. **65**: 437–453. doi:10.1002/lno.11315

Allen, A. E., M. H. Howard-Jones, M. G. Booth, M. E. Frischer, P. G. Verity, D. A. Bronk, and M. P. Sanderson. 2002. Importance of heterotrophic bacterial assimilation of ammonium and nitrate in the Barents Sea during summer. J. Mar. Syst. **38**: 93–108. doi:10.1016/S0924-7963(02)00171-9

Bayer, B., and others. 2016. Physiological and genomic characterization of two novel marine thaumarchaeal strains indicates niche differentiation. ISME J. **10**: 1051–1063. doi:10.1038/ismej.2015.200

Beman, J. M., B. N. Popp, and C. A. Francis. 2008. Molecular and biogeochemical evidence for ammonia oxidation by marine Crenarchaeota in the Gulf of California. ISME J. **2**: 429–441. doi:10.1038/ismej.2007.118

Berthelot, H., S. Duhamel, S. L'Helguen, J. F. Maguer, S. Wang, I. Cetinic, and N. Cassar. 2019. NanoSIMS single cell analyses reveal the contrasting nitrogen sources for small phytoplankton. ISME J. **13**: 651–662. doi:10.1038/s41396-018-0285-8

Berube, P. M., and others. 2015. Physiology and evolution of nitrate acquisition in *Prochlorococcus*. ISME J. **9**: 1195–1207. doi:10.1038/ismej.2014.211

Bradley, P. B., M. W. Lomas, and D. A. Bronk. 2010. Inorganic and organic nitrogen use by phytoplankton along Chesapeake Bay, measured using a flow cytometric sorting approach. Estuaries Coast. **33**: 971–984. doi:10.1007/s12237-009-9252-y

Bronk, D. A., and B. B. Ward. 2000. Magnitude of dissolved organic nitrogen release relative to gross nitrogen uptake in marine systems. Limnol. Oceanogr. **45**: 1879–1883. doi:10.4319/lo.2000.45.8.1879

Buchwald, C., and K. L. Casciotti. 2013. Isotopic ratios of nitrite as tracers of the sources and age of oceanic nitrite. Nat. Geosci. **6**: 308–313. doi:10.1038/NGEO1745

Casey, J. R., M. W. Lomas, J. Mandecki, and D. E. Walker. 2007. *Prochlorococcus* contributes to new production in the Sargasso Sea deep chlorophyll maximum. Geophys. Res. Lett. **34**: L10604. doi:10.1029/2006GL028725

Chavez, F. P., K. R. Buck, R. R. Bidigare, D. M. Karl, D. Hebel, M. Latasa, L. Campbell, and J. Newton. 1995. On the chlorophyll a retention properties of glass-fiber GF/F filters. Limnol. Oceanogr. **40**: 428–433. doi:10.4319/lo.1995.40.2.0428

Chen, L., J. Ma, Y. Huang, M. Dai, and X. Li. 2015. Optimization of a colorimetric method to determine trace urea in seawater. Limnol. Oceanogr.: Methods **13**: 303–311. doi:10.1002/lom3.10026

Chen, Y. L. L. 2005. Spatial and seasonal variations of nitrate-based new production and primary production in the South China Sea. Deep-Sea Res. I Oceanogr. Res. Pap. **52**: 319–340. doi:10.1016/j.dsr.2004.11.001

Cherrier, J., J. E. Bauer, and E. Druffel. 1996. Utilization and turnover of labile dissolved organic matter by bacterial heterotrophs in eastern North Pacific surface waters. Mar. Ecol. Prog. Ser. **139**: 267–279. doi:10.3354/meps139267

Cho, B. C., and F. Azam. 1995. Urea decomposition by bacteria in the Southern California Bight and its implications for the mesopelagic nitrogen cycle. Mar. Ecol. Prog. Ser. **122**: 21–26. doi:10.3354/meps122021

Connelly, T. L., S. E. Baer, J. T. Cooper, D. A. Bronk, and B. Wawrik. 2014. Urea uptake and carbon fixation by marine pelagic bacteria and archaea during the Arctic summer and winter seasons. Appl. Environ. Microbiol. **80**: 6013–6022. doi:10.1128/AEM.01431-14

Dugdale, R., and J. Goering. 1967. Uptake of new and regenerated forms of nitrogen in primary productivity. Limnol. Oceanogr. **12**: 196–206. doi:10.4319/lo.1967.12.2.0196

Dugdale, R. C., A. Morel, A. Bricaud, and F. P. Wilkerson. 1989. Modeling new production in upwelling centers: A case study of modeling new production from remotely sensed temperature and color. J. Geophys. Res. Oceans **94**: 18119–18132. doi:10.1029/JC094iC12p18119

Eppley, R., J. Sharp, E. Renger, E. Perry, and E. Harrison. 1977. Nitrogen assimilation by phytoplankton and other microorganisms in the surface waters of the central North Pacific Ocean. Mar. Biol. **39**: 111–120. doi:10.1007/BF00386996

Eppley, R. W., and B. J. Peterson. 1979. Particulate organic matter flux and planktonic new production in the deep ocean. Nature **282**: 677–680. doi:10.1038/282677a0

Fawcett, S. E., M. W. Lomas, J. R. Casey, B. B. Ward, and D. M. Sigman. 2011. Assimilation of upwelled nitrate by small eukaryotes in the Sargasso Sea. Nat. Geosci. **4**: 717–722. doi:10.1038/NGEO1265

Flombaum, P., and others. 2013. Present and future global distributions of the marine cyanobacteria *Prochlorococcus* and *Synechococcus*. Proc. Natl. Acad. Sci. USA **110**: 9824–9829. doi:10.1073/pnas.1307701110

Fouilland, E., M. Gosselin, R. B. Rivkin, C. Vasseur, and B. Mostajir. 2007. Nitrogen uptake by heterotrophic bacteria and phytoplankton in Arctic surface waters. J. Plankton Res. **29**: 369–376. doi:10.1093/plankt/fbm022

Francis, C. A., K. J. Roberts, J. M. Beman, A. E. Santoro, and B. B. Oakley. 2005. Ubiquity and diversity of ammonia-oxidizing archaea in water columns and sediments of the ocean. Proc. Natl. Acad. Sci. USA **102**: 14683–14688. doi:10.1073/pnas.0506625102

Garcia, H. E., R. A. Locarnini, T. P. Boyer, and J. I. Antonov. 2006. World Ocean Database 2005, p. 1–396. *In* S. Levitus [ed.], Nutrients (phosphate, nitrate, silicate), v. 4. NOAA Atlas NESDIS 64. U.S. Government Printing Office.

Gasol, J. M., and X. A. Moran. 1999. Effects of filtration on bacterial activity and picoplankton community structure as assessed by flow cytometry. Aquat. Microb. Ecol. **16**: 251–264. doi:10.3354/ame016251

Goddard, M. R., and M. A. Bradford. 2003. The adaptive response of a natural microbial population to carbon- and nitrogen-limitation. Ecol. Lett. **6**: 594–598. doi:10.1046/j.1461-0248.2003.00478.x

Han, A., M. Dai, S.-J. Kao, J. Gan, Q. Li, L. Wang, W. Zhai, and L. Wang. 2012. Nutrient dynamics and biological consumption in a large continental shelf system under the influence of both a river plume and coastal upwelling. Limnol. Oceanogr. **57**: 486–502. doi:10.4319/lo.2012.57.2.0486

Herlemann, D. P., M. Labrenz, K. Jürgens, S. Bertilsson, J. J. Waniek, and A. F. Andersson. 2011. Transitions in bacterial communities along the 2000 km salinity gradient of the Baltic Sea. ISME J. **5**: 1571–1579. doi:10.1038/ismej.2011.41

Holmes, R. M., J. W. McClelland, D. M. Sigman, B. Fry, and B. J. Peterson. 1998. Measuring ^{15}N-NH$_4^+$ in marine, estuarine and fresh waters: An adaptation of the ammonia diffusion method for samples with low ammonium concentrations. Mar. Chem. **60**: 235–243. doi:10.1016/S0304-4203(97)00099-6

Hopkinson, C. S., and J. J. Vallino. 2005. Efficient export of carbon to the deep ocean through dissolved organic matter. Nature **433**: 142–145. doi:10.1038/nature03191

Hu, A., N. Jiao, R. Zhang, and Z. Yang. 2011. Niche partitioning of marine group I Crenarchaeota in the euphotic and upper mesopelagic zones of the East China Sea. Appl. Environ. Microbiol. **77**: 7469–7478. doi:10.1128/AEM.00294-11

Hungate, B. A., R. L. Mau, E. Schwartz, J. G. Caporaso, P. Dijkstra, N. Van Gestel, and L. B. Price. 2015. Quantitative microbial ecology through stable isotope probing. Appl. Environ. Microbiol. **81**: 7570–7581. doi:10.1128/AEM.02280-15

Jacquet, S., H. Havskum, T. E. Thingstad, and D. Vaulot. 2002. Effects of inorganic and organic nutrient addition on coastal microbial community (Isefjord, Denmark). Mar. Ecol. Prog. Ser. **228**: 3–14. doi:10.3354/meps228003

Karner, M. B., E. F. DeLong, and D. M. Karl. 2001. Archaeal dominance in the mesopelagic zone of the Pacific Ocean. Nature **409**: 507–510. doi:10.1038/35054051

Key, R. M., and others. 2004. A global ocean carbon climatology: Results from Global Data Analysis Project (GLODAP). Global Biogeochem. Cycles **18**: 1–23. doi:10.1029/2004GB002247

Kirchman, D. L. 2002. Inorganic nutrient use by marine microorganisms. *In* G. Bitton [ed.], Encyclopedia of environmental microbiology. Wiley.

Kirchman, D. L., R. G. Keil, and P. A. Wheeler. 1990. Carbon limitation of ammonium uptake by heterotrophic bacteria in the subarctic Pacific. Limnol. Oceanogr. **35**: 1258–1266. doi:10.4319/lo.1990.35.6.1258

Kirchman, D. L., and P. A. Wheeler. 1998. Uptake of ammonium and nitrate by heterotrophic bacteria and phytoplankton in the sub-Arctic Pacific. Deep-Sea Res. I Oceanogr. Res. Pap. **45**: 347–365. doi:10.1016/S0967-0637(97)00075-7

Klawonn, I., S. Bonaglia, M. J. Whitehouse, S. Littmann, D. Tienken, M. M. M. Kuypers, V. Brüchert, and H. Ploug. 2019. Untangling hidden nutrient dynamics: Rapid ammonium cycling and single-cell ammonium assimilation in marine plankton communities. ISME J. **13**: 1960–1974. doi:10.1038/s41396-019-0386-z

Knapp, A. N., D. M. Sigman, and F. N. Lipschultz. 2005. N Isotopic composition of dissolved organic nitrogen and nitrate at the Bermuda Atlantic Time-series Study site. Global Biogeochem. Cycles **19**: 1–15. doi:10.1029/2004GB002320

Kozich, J. J., S. L. Westcott, N. T. Baxter, S. K. Highlander, and P. D. Schloss. 2013. Development of a dual-index sequencing strategy and curation pipeline for analyzing amplicon sequence data on the MiSeq Illumina sequencing platform. Appl. Environ. Microbiol. **79**: 5112–5120. doi:10.1128/AEM.01043-13

Large, W. G., and S. G. Yeager. 2008. The global climatology of an interannually varying air–sea flux data set. Clim. Dyn. **33**: 341–364. doi:10.1007/s00382-008-0441-3

Lomas, M. W., and F. Lipschultz. 2006. Forming the primary nitrite maximum: Nitrifiers or phytoplankton? Limnol. Oceanogr. **51**: 2453–2467. doi:10.4319/lo.2006.51.5.2453

Marie, D., F. Partensky, D. Vaulot, and C. Brussaard. 2001. Enumeration of phytoplankton, bacteria, and viruses in marine samples. Curr. Protoc. Cytom. **10**: 11.11.1–11.11.15. doi:10.1002/0471142956.cy1111s10

Martiny, A. C., S. Kathuria, and P. M. Berube. 2009. Widespread metabolic potential for nitrite and nitrate assimilation among *Prochlorococcus* cotypes. Proc. Natl. Acad. Sci. USA **106**: 10787–10792. doi:10.1073/pnas.0902532106

Middelburg, J. J., and J. Nieuwenhuize. 2000. Nitrogen uptake by heterotrophic bacteria and phytoplankton in the nitrate-rich Thames estuary. Mar. Ecol. Prog. Ser. **203**: 13–21. doi:10.3354/meps203013

Moir, J. W., and N. J. Wood. 2001. Nitrate and nitrite transport in bacteria. Cell. Mol. Life Sci. **58**: 215–224. doi:10.1007/PL00000849

Moore, J. K., S. C. Doney, and K. Lindsay. 2004. Upper ocean ecosystem dynamics and iron cycling in a global three-dimensional model. Global Biogeochem. Cycles **18**: 1–21. doi:10.1029/2004GB002220

Moore, L. R. 2002. Utilization of different nitrogen sources by the marine cyanobacteria *Prochlorococcus* and *Synechococcus*. Limnol. Oceanogr. **47**: 989–996. doi:10.4319/lo.2002.47.4.0989

Morando, M., and D. G. Capone. 2016. Intraclade heterogeneity in nitrogen utilization by marine prokaryotes revealed using stable isotope probing coupled with tag sequencing (Tag-SIP). Front. Microbiol. **7**: 1932. doi:10.3389/fmicb.2016.01932

Morando, M., and D. G. Capone. 2018. Direct utilization of organic nitrogen by phytoplankton and its role in nitrogen cycling within the Southern California Bight. Front. Microbiol. **9**: 2118. doi:10.3389/fmicb.2018.02118

Morel, A., Y. H. Ahn, F. Partensky, D. Vaulot, and H. Claustre. 1993. *Prochlorococcus* and *Synechococcus*: A comparative study of their optical properties in relation to their size and pigmentation. J. Mar. Res. **51**: 617–649. doi:10.1357/0022240933223963

Mulholland, M. R., and M. W. Lomas. 2008. Nitrogen uptake and assimilation, p. 303–384. *In* D. Capone, D. Bronk, M. Mulholland, and E. Carpenter [eds.], Nitrogen in the marine environment. Academic Press.

Nercessian, O., E. Noyes, M. G. Kalyuzhnaya, M. E. Lidstrom, and L. Chistoserdova. 2005. Bacterial populations active in metabolism of C_1 compounds in the sediment of Lake Washington, a freshwater lake. Appl. Environ. Microbiol. **71**: 6885–6899. doi:10.1128/AEM.71.11.6885-6899.2005

Neufeld, J. D., H. Schäfer, M. J. Cox, R. Boden, I. R. McRonald, and J. C. Murrell. 2007. DNA stable-isotope probing. Nat. Protoc. **2**: 860–866. doi:10.1038/nprot.2007.109

Park, J. W., and D. E. Crowley. 2005. Normalization of soil DNA extraction for accurate quantification of target genes by real-time PCR and DGGE. Biotechniques **38**: 579–586. doi:10.2144/05384ST04

Qin, W., and others. 2014. Marine ammonia-oxidizing archaeal isolates display obligate mixotrophy and wide ecotypic variation. Proc. Natl. Acad. Sci. USA **111**: 12504–12509. doi:10.1073/pnas.1324115111

Radajewski, S., P. Ineson, N. R. Parekh, and J. C. Murrell. 2000. Stable-isotope probing as a tool in microbial ecology. Nature **403**: 646–649. doi:10.1038/35001054

Seyler, L. M., L. R. McGuinness, J. A. Gilbert, J. F. Biddle, D. Gong, and L. J. Kerkhof. 2018. Discerning autotrophy, mixotrophy and heterotrophy in marine TACK archaea from the North Atlantic. FEMS Microbiol. Ecol. **94**: fiy014. doi:10.1093/femsec/fiy014

Shiozaki, T., T. Kodama, S. Kitajima, M. Sato, and K. Furuya. 2013. Advective transport of diazotrophs and importance of their nitrogen fixation on new and primary production in the western Pacific warm pool. Limnol. Oceanogr. **58**: 49–60. doi:10.4319/lo.2013.58.1.0049

Solomon, C. M., J. L. Collier, G. M. Berg, and P. M. Glibert. 2010. Role of urea in microbial metabolism in aquatic systems: A biochemical and molecular review. Aquat. Microb. Ecol. **59**: 67–88. doi:10.3354/ame01390

Takai, K., and K. Horikoshi. 2000. Rapid detection and quantification of members of the archaeal community by quantitative PCR using fluorogenic probes. Appl. Environ. Microbiol. **66**: 5066–5072. doi:10.1128/AEM.66.11.5066-5072.2000

Trottet, A., C. Leboulanger, F. Vidussi, R. Pete, M. Bouvy, and E. Fouilland. 2016. Heterotrophic bacteria show weak competition for nitrogen in Mediterranean coastal waters (Thau Lagoon) in autumn. Microb. Ecol. **71**: 304–314. doi:10.1007/s00248-015-0658-8

Wan, X. S., and others. 2018. Ambient nitrate switches the ammonium consumption pathway in the euphotic ocean. Nat. Commun. **9**: 915. doi:10.1038/s41467-018-03363-0

Wang, F. H., M. Qiao, J. Q. Su, Z. Chen, X. Zhou, and Y. G. Zhu. 2014. High throughput profiling of antibiotic resistance genes in urban park soils with reclaimed water irrigation. Environ. Sci. Technol. **48**: 9079–9085. doi:10.1021/es502615e

Wawrik, B., W. B. Boling, J. D. Van Nostrand, J. Xie, J. Zhou, and D. A. Bronk. 2012. Assimilatory nitrate utilization by bacteria on the West Florida Shelf as determined by stable isotope probing and functional microarray analysis. FEMS Microbiol. Ecol. **79**: 400–411. doi:10.1111/j.1574-6941.2011.01226.x

Widner, B., and M. R. Mulholland. 2017. Cyanate distribution and uptake in North Atlantic coastal waters. Limnol. Oceanogr. **62**: 2538–2549. doi:10.1002/lno.10588

Widner, B., C. A. Fuchsman, B. X. Chang, G. Rocap, and M. R. Mulholland. 2018. Utilization of urea and cyanate in waters overlying and within the eastern tropical north Pacific oxygen deficient zone. FEMS Microbiol. Ecol. **94**: fiy138. doi:10.1093/femsec/fiy138

Xu, M. N., Y. Wu, L. W. Zheng, Z. Zheng, H. Zhao, E. A. Laws, and S. J. Kao. 2017. Quantification of multiple simultaneously occurring nitrogen flows in the euphotic ocean. Biogeosciences **14**: 1021–1038. doi:10.5194/bg-14-1021-2017

Zhang, C. L., W. Xie, A. B. Martin-Cuadrado, and F. Rodriguez-Valera. 2015. Marine Group II Archaea, potentially important players in the global ocean carbon cycle. Front. Microbiol. **6**: 1108. doi:10.3389/fmicb.2015.01108

Zhang, Y., N. Jiao, and N. Hong. 2008. Comparative study of picoplankton biomass and community structure in different provinces from subarctic to subtropical oceans. Deep-Sea Res. II Top. Stud. Oceanogr. **55**: 1605–1614. doi:10.1016/j.dsr2.2008.04.014

Zhang, Y., W. Deng, X. Xie, and N. Jiao. 2016. Differential incorporation of carbon substrates among microbial populations identified by field-based, DNA stable-isotope probing in South China Sea. PLoS One **11**: e0157178. doi:10.1371/journal.pone.0157178

Zhu, F., R. Massana, F. Not, D. Marie, and D. Vaulot. 2005. Mapping of picoeucaryotes in marine ecosystems with quantitative PCR of the 18S rRNA gene. FEMS Microbiol. Ecol. **52**: 79–92. doi:10.1016/j.femsec.2004.10.006

Acknowledgments

Conflict of Interest

None declared.